The exchange interaction effects on magnetic properties of the nanostructured CoPt particles

S.V. Komogortsev[1,*] , R.S. Iskhakov[1] , A.A. Zimin[4], E.Yu. Filatov[2,3] , S.V. Korenev[2,3] , Yu.V. Shubin[2,3] , N.A. Chizhik[4] , G.Yu. Yurkin[1] , E.V. Eremin[1]

[1]Kirensky Institute of Physics, SB RAS, 660036 Krasnoyarsk, Russia

[2]Nikolaev Institute of Inorganic Chemistry SB RAS, 630090 Novosibirsk, Russia

[3]Novosibirsk State University, 630090 Novosibirsk, Russia

[4]Siberian Federal University, 660041 Krasnoyarsk, Russia

* Corresponding author: komogor@iph.krasn.ru

Abstract

Various manifestations of the exchange interaction effects in magnetization curves of the CoPt nanostructured particles are demonstrated and discussed. The inter-grain exchange constant A in the sponge-like agglomerates of crystallites is estimated as $A = (7 \pm 1)$ pJ/m from the approach magnetization to saturation curves that is in good agreement with $A = (6.6 \pm 0.5)$ pJ/m obtained from Bloch $T^{3/2}$ law. The fractal dimensionality of the exchange coupled crystallite system in the porous media of the disordered CoPt alloy $d = (2.60 \pm 0.18)$ was estimated from the approach magnetization to saturation curve. Coercive force decreases with temperature as $H_c \sim T^{3/2}$ which is assumed to be a consequence of the magnetic anisotropy energy reduction due to the thermal spin wave excitations in the investigated CoPt particles.

Introduction

Ordered fct ($L1_0$) CoPt alloy is well-known for its chemical inertness and remarkable hard magnetic properties. The combination of these properties is highly desirable for permanent nanomagnets used in magnetic recording and biomedicine [1–3]. Coercive force, remanence and energy product of isolated homogeneous CoPt nanomagnets is determined by saturation magnetization and by magnitude and symmetry of the magnetic anisotropy energy. In practice, both individual nanocrystals and CoPt particle-based media are characterized by various structural and phase imperfections: different crystallographic orientations of the crystallites in thin films and nanostructured alloys, phase composition inhomogeneity resulting from the alternation of the ordered and disordered solid solution regions, antiphase and twin boundaries, etc. These imperfections could be used to raise the coercivity due to domain wall pinning center concentration increase in films [4–6] and could also raise remanence as a consequence of the exchange interaction between nanophase regions of the CoPt ordered and disordered solid solution [7–12]. In general, magnetic microstructure of the structurally inhomogeneous media is significantly influenced by the exchange interaction leading to the formation of the magnetically ordered regions with the characteristic length scale exceeding the typical size of structural imperfections [13–19]. The effective magnetic anisotropy and the hysteresis loop shape would then be determined by the intergrain exchange interaction [18–20]. Qualitative investigation of the intercrystallite, intergrain or interphase interactions is frequently performed using the so called remanence magnetization curves or Henkel plots [21–27]. These methods are suitable for the weak interparticle ineractions case. However, they are sometimes used to estimate the interactions between crystallites in the polycrystalline media [25,28,29]. The measurement of the Curie temperature in the intergranular phase of two-phase material is also used for evaluation of the intergranular exchange [30]. It is impossible to use it in the nanostructured CoPt particles, because at temperatures comparable to the Curie temperature they undergo structural transformations and their crystallites grow [31].

We will demonstrate in this paper an alternative approach to the investigation of the exchange interaction effect on the approach of magnetization to saturation curve in the nanostructured CoPt particles. In that case intercrystalline interactions are significant and comparable to the intragrain interactions. This approach allows us to estimate quantitatively the exchange interaction between crystallites and volume-averaged exchange over the whole sample.

Experiment

The samples of equiatomic CoPt nanoparticles were prepared by thermal decomposition of the precursor compound $[Pt(NH_3)_4][Co(C_2O_4)_2(H_2O)_2]\cdot 2H_2O$ [32]. As-decomposed particles were then annealed in helium atmosphere at 400ºC, 500ºC and 600ºC during 2, 4, 8 and 16 hours. Metal nanocrystalline powder was studied over the 2θ range 5–120º on a DRON RM4 powder diffractometer equipped with a Cu Kα source (λ = 1.5418 Å) and a graphite monochromator for the diffracted beam.

Powder diffraction patterns were measured at Cu Ka radiation. For further line profile analysis, instrumental profile was measured using the coarse Si powder. We have not found any increase in accuracy using the fine structure profile of the Cu K_α doublet as proposed by Berger [33], so we are using just $K_{\alpha 1/\alpha 2}$ doublet in further modeling.

In order to perform the line profile analysis of the as-decomposed at 400°C CoPt nanoparticles we have used the whole powder pattern modeling (WPPM) procedure described by P. Scardi and M. Leoni [34] using its implementation in the PM2K package [35]. The key difference between WPPM and well-known Rietveld method [36] is that in WPPM method line profile is modeled directly in terms of physically meaningful parameters, such as particle size distribution, dislocation density, stacking/twin fault probability. However, peak intensity has no direct physical meaning in WPPM. In the Rietveld method one has to use an arbitrary line profile model with a possibility to refine structural parameters in terms of peak width dependence on the scattering vector, and peak intensity has direct physical meaning. Rietveld method is associated

with well-known line profile analysis methods, such as Williamson-Hall or Warren-Averbach plots with a variety of modifications, but all these model have to rely on peak width determined using arbitrary bell-shaped function. WPPM approach is superior to these methods.

Magnetic measurements were made by SQUID magnetometer on the base of MPMS and vibrating sample magnetometer (VSM) PPMS - Quantum Design magnetometers. The powder sample was fixed in the wax matrix to avoid particle displacement in VSM cell. Wax used to fix the powder is characterized by small paramagnetic response. This signal was measured separately and then subtracted.

Results and discussion

XRD and TEM investigation of the CoPt particles reveals the following: individual CoPt powder particle is a sponge-like agglomerate of nanocrystallites (Fig. 2). The nanocristallite size is about few nanometers, while the size of the whole agglomerate could exceed 500 nm.

X-ray powder diffraction patterns for selected CoPt samples during annealing at 400°C and 500°C are shown on the figure 2. The amount of $L1_0$ phase increases as annealing time is increased, occurring faster at 500°C. Peak breadth also decreases as annealing proceeds, indicating formation of larger crystallites. We need the structural data and crystallite sizes for further discussion. The best fit shown on fig. 3 corresponds to the FCC disordered CoPt solid solution phase with average crystallite size determined to be $D = (2.7 \pm 0.1)$ nm. These 0.1 nm error is related to the least-squares estimation of the particle size distribution parameters by fitting the lognormal distribution to the XRPD pattern, but of course it does not indicate the monodispersity of the sample up to an angstrom. Crystallite is defined as a coherently scattering domain and is unrelated to the observed on the TEM images nanometer sized aggregates of crystallites. Crystallites may contain both ordered $L1_0$ and disordered A1 regions [37].

The hysteresis loop shape transforms during annealing, with increasing coercivity H_c and squareness M_r/M_s (Fig. 4). The coercivity growth is observed up to 16 h of annealing at 500 °C

($\mu_0 \cdot H_c$ = 1.42 T) and up to 8 h of annealing at 600 °C ($\mu_0 \cdot H_c$ = 1.37 T) followed by decrease after annealing at 600 °C during 16 h ($\mu_0 \cdot H_c$ = 0.82 T). Squareness of the loop (M_r/M_s) has increased after the first stages of annealing and stays at the 0.70 ± 0.05 level afterwards.

Structurally inhomogeneous crystallites with the size less than 10 nm have almost uniform magnetization [38]. In this case one can characterize crystallite using single easy magnetization axis [38]. In the ensemble of non-interacting uniaxial crystallites M_r/M_s = 0.5 is expected [39]. Remanence enhancement is usually attributed to the intercrystallite exchange interaction effects [9,40]. Estimation of the magnitude of these exchange interaction effects could be performed by the analysis of the approach magnetization to saturation curves [17]. However, the analysis could be done only in the reversible high-field regime. This condition is completely satisfied in case of as-prepared CoPt sample, and its magnetization curve in the approach to saturation regions is shown at Fig. 5 in double logarithmic scale in order to visualize power-law behavior of the $M(H)$ curve. Note the change from $M(H) \sim H^{-0.7}$ in the vicinity of H_R below 3 T to the $M(H) \sim H^{-2}$ behavior above 3 T . This is how magnetization is expected to approach saturation in the exchange-coupled system of randomly oriented crystallites [13,14,17,41].

According to [13,17,42] the high- and low-field regime for the approach magnetization to saturation law should be distinguished. Magnetization curve in $H > H_R = 2A/M_s \cdot R_c^2$ range is determined solely by competition between the energy of the external magnetic field with the magnetic anisotropy energy and thus allows to determine the latter from the experimental $M(H)$ curve by fitting it with Eq.(1) [13,17,42–44]:

$$M(H) = M_s \left[1 - \frac{2}{105} \cdot \left(\frac{2 \cdot K}{M_s \cdot H} \right)^2 \right], \qquad (1)$$

Here A is the exchange constant, R_c is ‘‘structural correlation length’’ or the average crystallite size $D = R_c$, M_s is saturation magnetization, K is magnetic anisotropy constant in crystallite. The factor of 2/105 in the eq. (1) corresponds to the cubic magnetic anisotropy in the FCC CoPt crystallites. By fitting *M(H)* in the eq. (1) in the field range from 3.5 to 5 T (where according to

fig. 5 the $M(H) \sim H^{-2}$ relation holds) and using $M_s = (0.67 \pm 0.03)$ MA/m, we have estimated $K = (2.4 \pm 0.2) \cdot 10^5$ J/m^3.

Because the exchange field is defined as $\mu_0 \cdot H_R = 2A/M_s \cdot R_c^2$, we use it to estimate A [13,45–47]. Using $\mu_0 \cdot H_R = (3.0 \pm 0.1)$ T (according to fig. 5), $M_s = (0.67 \pm 0.03)$ MA/m, and the crystallite size $D = (2.7 \pm 0.1)$ nm determined from XRD for CoPt particles, we estimate exchange constant A as $A = (\mu_0 \cdot H_R \cdot M_s) \cdot D^2/2$. The result is $A = (7 \pm 1) \cdot$ pJ/m.

According to [14,17,41,48], in materials with randomly oriented local easy magnetization axis approach to saturation behavior below the H_R is:

$$M(H) = M_s \cdot (1 - c_\alpha \cdot H^{-\alpha}) \qquad (2)$$

The exponent here is $\alpha = (4 - d)/2$ and it depends on the dimensionality of the exchange coupled crystallites system [14,17,41,48]. The value of the exponent obtained as a result of *M(H)* fitting in the field range from 0.5 to 2 T (where according to fig. 5 power law $M(H) \sim H^{-\alpha}$ holds) is estimated to be $\alpha = (0.70 \pm 0.05)$. The corresponding dimensionality could then be estimated as $d = (2.60 \pm 0.18)$. The determination of the dimensionality is far from trivial when it comes to sponge-like structures whose fractal dimensionality may well have non-integer value.

The fractal dimensionality d estimated there is an average over large number of exchange coupled volumes with uniform orientation of local easy magnetization axis. In nanostructured media this volume naturally corresponds to a crystallite. Dimensionality in this case is determined as $d = \ln(N)/\ln(L_m/D)$, where N is the number of crystallites with size (D) inside the magnetic correlation length (L_m). It is assumed that the magnetization of the coupled crystallites with size ($D \approx 2.7$ nm) is correlated on a length scale $L_m > D$. This assumption is justified in our case, because it is the necessary condition to observe the $M(H) \sim \cdot H^{-\alpha}$ power law in the fields below H_R [17,41,45]. What is more, this assumption can be verified quantitatively. According to the random magnetic anisotropy model L_m can be estimated as $L_m = \delta \cdot (\delta/D)^{d/(4-d)}$, where $\delta = \sqrt{\frac{A}{K}}$ [13,41,49]. Using previously determined exchange constant A, anisotropy constant K, crystallite

size D and dimensionality d we obtain an estimation for the $L_m \approx 20$ nm. It follows that $N > 1$, and L_m contains several crystallites of size D. In the high field region (approach of the magnetization to saturation) L_m decreases as field increases, and approaches D as field approaches H_R. This is the underlying physics behind the model in eq. (2) [17,50]. The dimensionality determined in this way characterizes the scale invariance of the nanostructured media on a length scale from 3 to 20 nm.

Note also that identification of the integer-valued dimensionalities of either the non-uniform anisotropy or magnetic correlations from the approach of magnetization to saturation is known in the literature for 2D, 3D and 1D systems of exchange coupled grains [14,17,41,51–53]. In the paper [54] fractal dimensionality of the nanogranulated medium near the magnetic percolation threshold was estimated using the same approach. We assume that the deviation of the dimensionality determined in this paper from the integer values is related to the nanoporosity of the medium. The point is that presence of pores decreases the number of crystallites N in the volume with size L_m, and finally for fixed L_m and D the resulting $d = \ln(N)/\ln(L_m/D)$ is lower than in the continuous medium, where $d = 3$. Estimation for $d = (2.60 \pm 0.18)$ for medium shown on fig. 1 thus seems to be plausible.

Another way usually used for exchange constant determination is fitting $M(T)$ dependence in low temperatures by Bloch $T^{3/2}$ law [55]:

$$M(T) = M_0\left(1 - 2.612\left(\frac{M_0 \cdot \rho}{g\mu_B}\right)^{1/2} \cdot \left(\frac{k_B T}{8\pi A}\right)^{3/2}\right). \qquad (3)$$

Temperature dependence of magnetization in as-prepared CoPt sample is well fitted by Eq.3 (Fig.6): Were $A = (6.6 \pm 0.5)$ pJ/m, $M_0 = (42 \pm 2)$ A·m^2/kg and $\rho = 16040$ kg m^{-3} for CoPt. Note that exchange constants estimated in two different approaches are in good agreement. The deviation from the Bloch law below 50 K similar to that in our fig.4 in the low temperature range were recently connected to the Bose-Einstein condensation of magnons in the nanostructured

ferromagnetic [56]. Another explanation is the possibility of the contributions arising from the small particles, which are isolated from the agglomerate. For isolated CoPt nanoparticles with sizes about 4 nm and below paramagnetic-like response is possible, which is related to the temperature-activated particle remagnetization process [57].

In small particles H_c could be decreased significantly due to thermal destabilization of the magnetic moment of a particle. In nanostructured media it is possible to overcome this effect due to the increase of the activation volume of the field-switched region resulting from the exchange interaction between crystallites. Coercivity of our particles decreases slightly in the temperature range 5 – 200 K and follows $T^{3/2}$ law (Fig.7): $H_c \sim H_{c0} \cdot (1\text{-}C \cdot T^{3/2})$. This dependence is expected for single-domain ferromagnetic nanoparticles, where H_c is related to the magnetic anisotropy energy as $H_c \sim 2K/M_s$ and thermal-activated switching doesn't mean. According to the single-ion anisotropy theory $K \sim M^n$ [55]. Taking into account that in ferromagnetic materials in low temperatures magnetization decreases with temperature according to Eq.3 and $B \cdot T^{3/2} << 1$ the following relation could be obtained: $H_c \sim H_a \sim M^{n-1} \approx M_0 \cdot (1\text{-}B \cdot (n\text{-}1) \cdot T^{3/2})$. In addition, slight decrease in H_c with T allows extrapolation of the conclusions concerned with the exchange interaction influence on the hysteresis loop shape to the near-room temperatures.

Acknowledgments

The work has been supported by RFBR Grant 12-02-00943-a, 11-03-00168-a, Interdisciplinary integration of fundamental research of SB RAS (2012-2014)- project 64.

Conclusions

The effects of the exchange interaction on the approach of magnetization to saturation curve of the CoPt nanostructured particles are demonstrated and discussed. The investigation of approach

magnetization to saturation curves provides dimensionality d of exchange coupled crystallite system and inter-grain exchange stiffness constant A: $d = (2.60 \pm 0.18)$ and $A = (7 \pm 1)$ pJ/m that is in good agreement with $A = (6.6 \pm 0.5)$ pJ/m obtained from Bloch $T^{3/2}$ law. Coercive force decreases with temperature as $H_c \sim T^{3/2}$ which could result from the magnetic anisotropy energy reduction due to the thermal spin wave excitations in the investigated CoPt particles.

References

[1] A. Alam, B. Kraczek, D. Johnson, Structural, magnetic, and defect properties of Co-Pt-type magnetic-storage alloys: Density-functional theory study of thermal processing effects, Phys. Rev. B. 82 (2010) 024435.

[2] H. Sato, I. Kaitsu, I. Okamoto, Magnetic storage madium, US 6,534,205 B2, 2003.

[3] E. Kita, T. Oda, T. Kayano, S. Sato, M. Minagawa, H. Yanagihara, et al., Ferromagnetic nanoparticles for magnetic hyperthermia and thermoablation therapy, J. Phys. D. Appl. Phys. 43 (2010) 474011.

[4] K. Belashchenko, V. Antropov, Multiscale nature of hysteretic phenomena: Application to CoPt-type magnets, Phys. Rev. B. 66 (2002) 144402.

[5] N. Vlasova, G.S. Kandaurova, N.N. Shchegoleva, Effect of the polytwinned microstructure parameters on magnetic domain structure and hysteresis properties of the CoPt-type alloys, J. Magn. Magn. Mater. 222 (2000) 138–158.

[6] B. Zhang, W.A. Soffa, Magnetic domains and coercivity in polytwinned ferromagnets, Phys. Status Solidi. 131 (1992) 707–725.

[7] Q.F. Xiao, E. Brück, Z.D. Zhang, F.R. de Boer, K.H.J. Buschow, Phase transformation and magnetic properties of bulk CoPt alloy, J. Alloys Compd. 364 (2004) 64–71.

[8] Q.F. Xiao, E. Brück, Z.D. Zhang, F.R. de Boer, K.H.J. Buschow, Effect of exchange coupling in nanocrystalline CoPt bulk magnets, J. Appl. Phys. 91 (2002) 8819.

[9] Q.F. Xiao, E. Brück, Z.D. Zhang, F.R. de Boer, K.H.J. Buschow, Remanence enhancement and coercivity in two-phase CoPt bulk magnets, J. Appl. Phys. 91 (2002) 304.

[10] Q.F. Xiao, E. Brück, Z.D. Zhang, F.R.D. Boer, K.H.J. Buschov, Remanence enhancement in nanocrystalline CoPt bulk magnets, J. Alloys Compd. 336 (2002) 41–45.

[11] H. Kronmüller, R. Fischer, M. Seeger, A. Zern, Micromagnetism and microstructure of hard magnetic materials, J. Phys. D. Appl. Phys. 29 (1996) 2274–2283.

[12] T. Schrefl, J. Fidler, H. Kronmüller, Remanence and coercivity in isotropic nanocrystalline permanent magnets, Phys. Rev. B. 49 (1994) 6100–6110.

[13] E.M. Chudnovsky, W.M. Saslow, R.A. Serota, Ordering in ferromagnets with random anisotropy, Phys. Rev. B. 33 (1986) 251–261.

[14] R.S. Iskhakov, V.A. Ignatchenko, S. V Komogortsev, A.D. Balaev, Study of magnetic correlations in nanostructured ferromagnets by correlation magnetometry, J. Exp. Theor. Phys. Lett. 78 (2003) 646–650.

[15] J. Loffler, H. Braun, W. Wagner, Magnetic correlations in nanostructured ferromagnets, Phys. Rev. Lett. 85 (2000) 1990–3.

[16] A. Michels, R.N. Viswanath, J.G. Barker, R. Birringer, J. Weissmu, J. Weissmüller, Range of Magnetic Correlations in Nanocrystalline Soft Magnets, Phys. Rev. Lett. 91 (2003) 267204.

[17] R.S. Iskhakov, S. V Komogortsev, Magnetic microstructure of amorphous, nanocrystalline, and nanophase ferromagnets, Phys. Met. Metallogr. 112 (2011) 666–681.

[18] R. Skomski, D. Leslie-Pelecky, R.D. Kirby, A. Kashyap, D.J. Sellmyer, Coercivity of disordered nanostructures, Scr. Mater. 48 (2003) 857–862.

[19] R. Skomski, Nanomagnetics, J. Phys. Condens. Matter. 15 (2003) R841–R896.

[20] G. Herzer, Grain size dependence of coercivity and permeability in nanocrystalline ferromagnets, Magn. IEEE Trans. 26 (1990) 1397–1402.

[21] O. Henkel, Remanenzverhalten und Wechselwirkungen in hartmagnetischen Teilchenkollektiven, Phys. Status Solidi. 7 (1964) 919–929.

[22] P.E. Kelly, K. O'Grady, P.I. Mayo, R. Chantrell, Switching mechanisms in cobalt-phosphorus thin films, IEEE Trans. Magn. 25 (1989) 3881–3883.

[23] L.P. Ol'khovik, M.M. Khvorov, N.M. Borisova, Z. V. Golubenko, Z.I. Sizova, E. V. Shurinova, The influence of interparticle interaction on magnetization curves of nano-and microcrystal ensembles, Phys. Solid State. 45 (2003) 675–680.

[24] B. Rellinghaus, S. Stappert, M. Acet, E.F. Wasserman, Magnetic properties of FePt nanoparticles, J. Magn. Magn. Mater. 266 (2003) 142–154.

[25] L. Tao, L. Wei, L. Jiajie, Y. Aru, Z. Minggang, Investigation of interaction mechanisms in nanocomposite PtCo permanent magnetic alloy, J. Appl. Phys. 109 (2011) 07A751.

[26] Y. Gao, X. Zhang, Z. Yin, S. Qu, J. You, N. Chen, Magnetic Properties of FePt Nanoparticles Prepared by a Micellar Method., Nanoscale Res. Lett. 5 (2009) 1–6.

[27] J. Lyubina, K. Khlopkov, O. Gutfleisch, K.-H. Muller, L. Schultz, Intergrain interactions in nanocomposite Fe–Pt powders, J. Appl. Phys. 99 (2006) 08E903.

[28] V.G. Shadrov, L. V. Nemtsevich, Intercrystallite magnetic interactions and properties of nanostructured magnetic materials (review), Inorg. Mater. Appl. Res. 3 (2012) 48–57.

[29] R.W. Chantrell, K. O'Grady, Magnetic characterization of recording media, J. Phys. D. Appl. Phys. 25 (1992) 1–23.

[30] A. Hernando, I. Navarro, P. Gorría, Iron exchange-field penetration into the amorphous interphase of nanocrystalline materials, Phys. Rev. B. 51 (1995) 3281–3284.

[31] S. V Komogortsev, R.S. Iskhakov, A.A. Zimin, E.Y. Filatov, S. V Korenev, Y. V Shubin, et al., Magnetic anisotropy and order parameter in nanostructured CoPt particles, Appl. Phys. Lett. 103 (2013) 152404.

[32] A. Zadesenets, E. Filatov, P. Plyusnin, I. Baidina, V. Dalezky, Y. Shubin, et al., Bimetallic single-source precursors [M(NH3)4][Co(C2O4)2(H2O)2]•2H2O (M = Pd, Pt) for the one run synthesis of CoPd and CoPt magnetic nanoalloys, Polyhedron. 30 (2011) 1305–1312.

[33] H. Berger, Study of the Kα emission spectrum of copper, XRay Spectrom. 15 (1986) 241–243.

[34] P. Scardi, M. Leoni, Whole powder pattern modelling, Acta Crystallogr. Sect. A Found. Crystallogr. 58 (2002) 190–200.

[35] M. Leoni, T. Confente, P. Scardi, PM2K: A flexible program implementing Whole Powder Pattern Modelling, in: Zeitschrift Fur Krist. Suppl., 2006: pp. 249–254.

[36] H.M. Rietveld, A profile refinement method for nuclear and magnetic structures, J. Appl. Crystallogr. 2 (1969) 65–71.

[37] F. Tournus, K. Sato, T. Epicier, T.J. Konno, V. Dupuis, Multi-L1_{0} Domain CoPt and FePt Nanoparticles Revealed by Electron Microscopy, Phys. Rev. Lett. 110 (2013) 055501.

[38] N.A. Usov, J.M. Barandiarán, Effective magnetic anisotropy of annealed FePt nanoparticles, Appl. Phys. Lett. 101 (2012) 172402.

[39] E.C. Stoner, E.P. Wohlfarth, A mechanism of magnetic hysteresis in heterogeneous alloys, Phil.Trans. Roy. Soc. A. 240 (1948) 559.

[40] H. Kronmüller, R. Fischer, Micromagnetism and microstructure of hard magnetic materials, J. Phys. D. Appl. Phys. 29 (1996) 2274–2283.

[41] R.S. Iskhakov, S. V Komogortsev, A.D. Balaev, L.A. Chekanova, Dimensionality of a system of exchange-coupled grains and magnetic properties of nanocrystalline and amorphous ferromagnets, J. Exp. Theor. Phys. Lett. 72 (2000) 304–307.

[42] V.A. Ignatchenko, R.S. Iskhakov, G. V Popov, Law of approach to ferromagnetic saturation in amorphous ferromagnets, Sov. Phys. JETP. 55 (1982) 878–886.

[43] Y. Melikhov, J.E. Snyder, D.C. Jiles, A.P. Ring, J.A. Paulsen, C.C.H. Lo, et al., Temperature dependence of magnetic anisotropy in Mn-substituted cobalt ferrite, J. Appl. Phys. 99 (2006).

[44] A. Franco, F.L.A. MacHado, V.S. Zapf, Magnetic properties of nanoparticles of cobalt ferrite at high magnetic field, in: J. Appl. Phys., 2011.

[45] L. Thomas, J. Tuaillon, J.P. Perez, V. Dupuis, A. Perez, B. Barbara, Approach to saturation in nanocrystallized films of iron and nickel, J. Magn. Magn. Mater. 140-144 (1995) 437–438.

[46] J. Perez, V. Dupuis, J. Tuaillon, A. Perez, V. Paillard, P. Mellinon, et al., Magnetic properties of nanostructured iron films obtained by low energy neutral cluster beam deposition, J. Magn. Magn. Mater. 145 (1995) 74–80.

[47] V. Dupuis, J.P. Perez, J. Tuaillon, V. Paillard, P. Mélinon, A. Perez, et al., Magnetic properties of nanostructured thin films of transition metal obtained by low energy cluster beam deposition, J. Appl. Phys. 76 (1994) 6676.

[48] V.A. Ignatchenko, R.S. Iskhakov, The Magnetization Curve of Ferromagnets with Anisotropic and Low-Dimensional Inhomogeneities, Fiz. Met. Met. 73 (1992) 602–608.

[49] G. Herzer, Magnetization process in nanocrystalline ferromagnets, Mater. Sci. Eng. A. 133 (1991) 1–5.

[50] A. Michels, R. Viswanath, J. Barker, R. Birringer, J. Weissmüller, Range of Magnetic Correlations in Nanocrystalline Soft Magnets, Phys. Rev. Lett. 91 (2003) 267204.

[51] R.S. Iskhakov, S. V Komogortsev, A.D. Balaev, A. V Okotrub, A.G. Kudashov, V.L. Kuznetsov, et al., Fe nanowires in carbon nanotubes as an example of a one-dimensional system of exchange-coupled ferromagnetic nanoparticles, J. Exp. Theor. Phys. Lett. 78 (2003) 236–240.

[52] J. Ruiz, X. Zhang, C. Ferrater, J. Tejada, Evidence of extended orientational order in amorphous Fe/Sm thin films, Phys. Rev. B. 52 (1995) 10202–10206.

[53] C. Binns, M.J. Maher, Magnetic behaviour of thin films produced by depositing pre-formed Fe and Co nanoclusters, New J. Phys. 4 (2002) 85–85.

[54] R.S. Iskhakov, S. V Komogortsev, E.A. Denisova, Y.E. Kalinin, A. V Sitnikov, Fractal magnetic microstructure in the (Co41Fe39B20)x(SiO2)1−x nanocomposite films, JETP Lett. 86 (2007) 465–469.

[55] J.M.D. Coey, Magnetism and magnetic materials, Cambridge University Press, New York, 2010.

[56] E. Della Torre, L. Bennett, R. Watson, Extension of the Bloch T3/2 Law to Magnetic Nanostructures: Bose-Einstein Condensation, Phys. Rev. Lett. 94 (2005) 147210.

[57] V. Dupuis, N. Blanc, L.E. Diaz-Sanchez, A. Hillion, A. Tamion, F. Tournus, et al., Finite size effects on structure and magnetism in mass-selected CoPt nanoparticles, Eur. Phys. J. D. 67 (2013) 25.

Figures

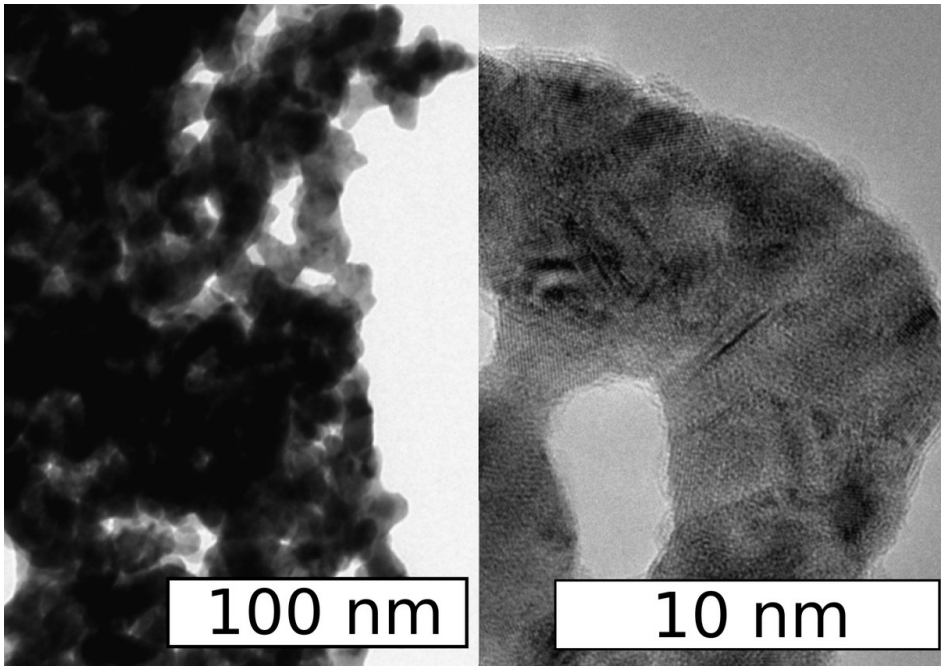

Fig.1 TEM images of the as-prepared nanostructured CoPt particles.

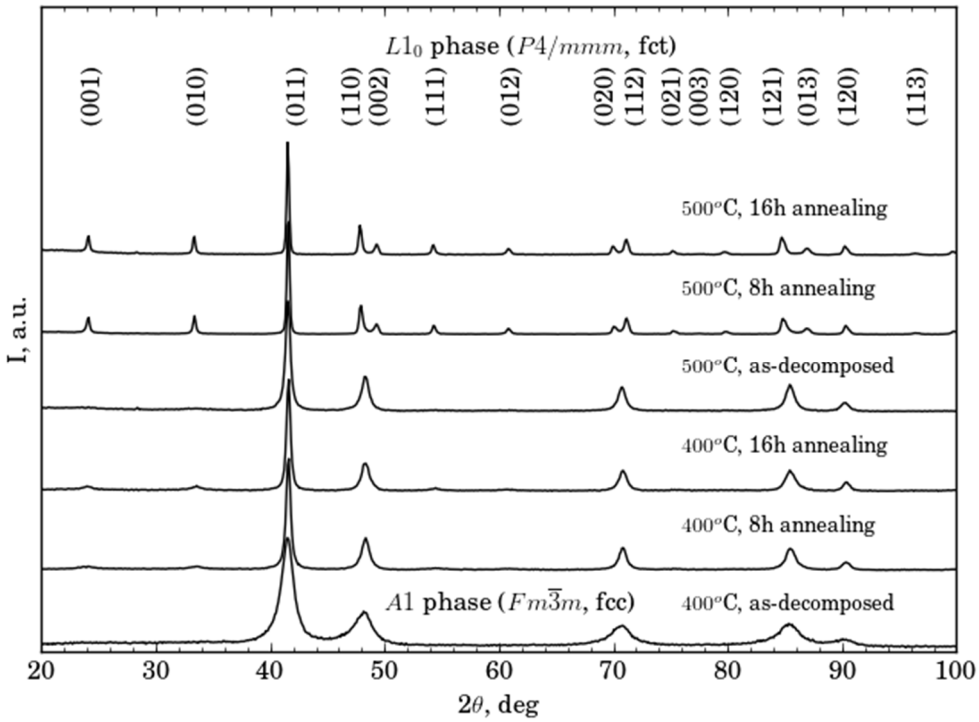

Fig. 2 X-ray powder diffraction patterns of the CoPt nanoparticles annealed at 400°C and 500°C with increased annealing time. Evolution of the diffraction patterns for given temperature with annealing time indicates formation of the L10 phase and decrease in width of the peaks.

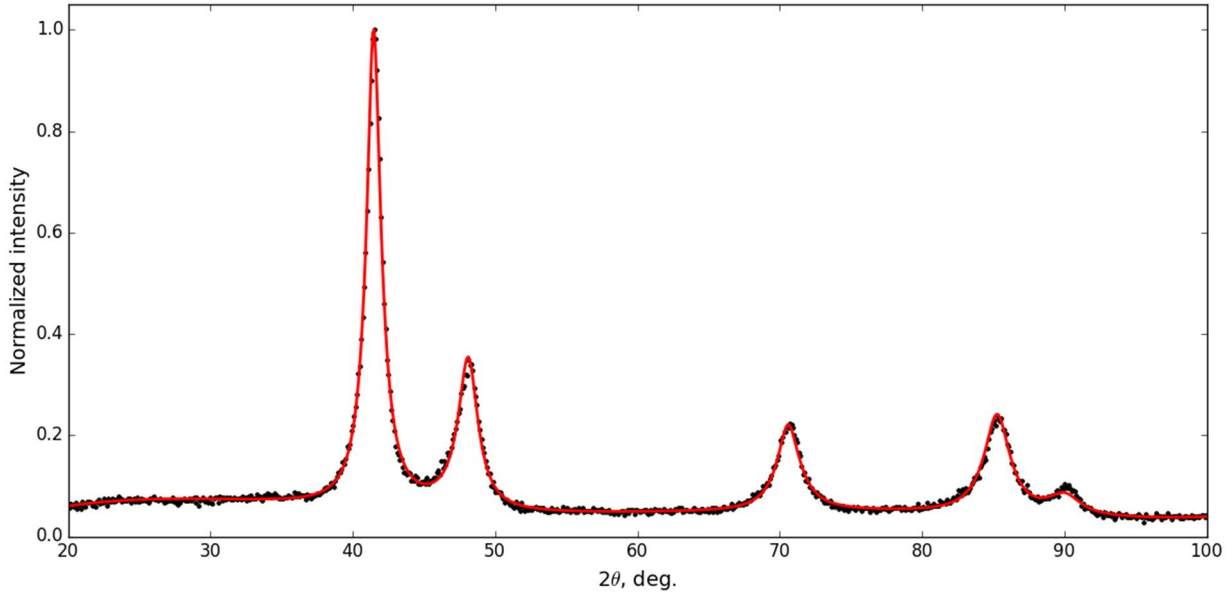

Fig.3 Experimental x-ray powder diffraction pattern of the as-decomposed at 400°C CoPt nanoparticles (black points) and the corresponding WPPM model (red line).

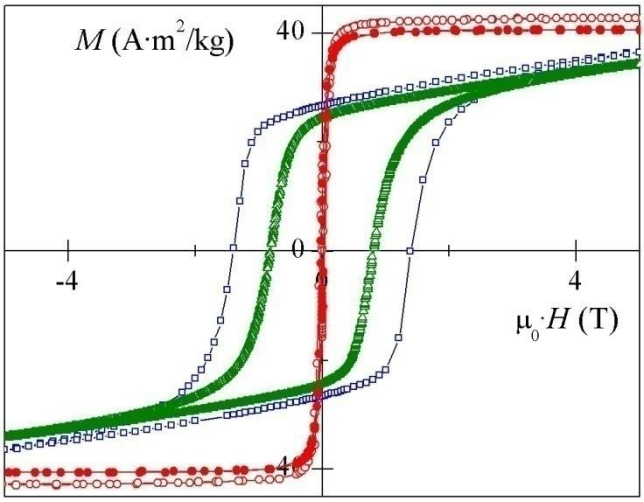

Fig.4 Transformation of the hysteresis loop measured at 5K in as-prepared and annealed CoPt particles. Red open circles – as prepared particles (red filled circles – loop measured at 300K), blue squares – annealed during 16 h at 500 °C, green triangles - annealed during 16 h at 600 °C.

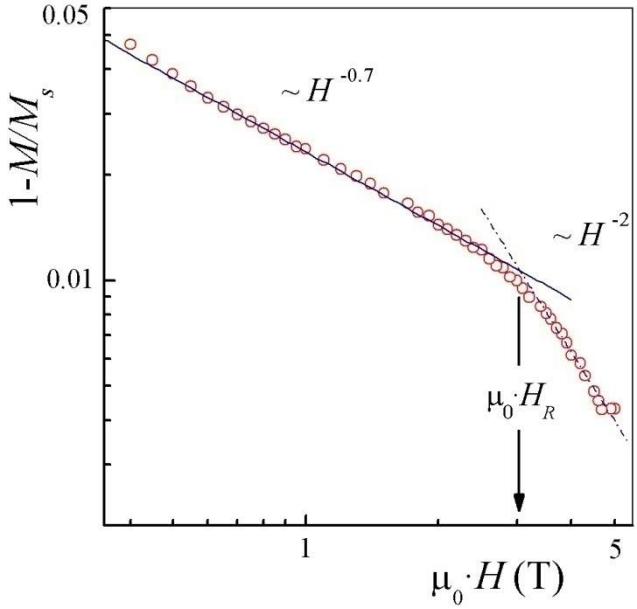

Fig.5 Field dependence of the magnetization for as-prepared particles near the saturation (double logarithmic scale).

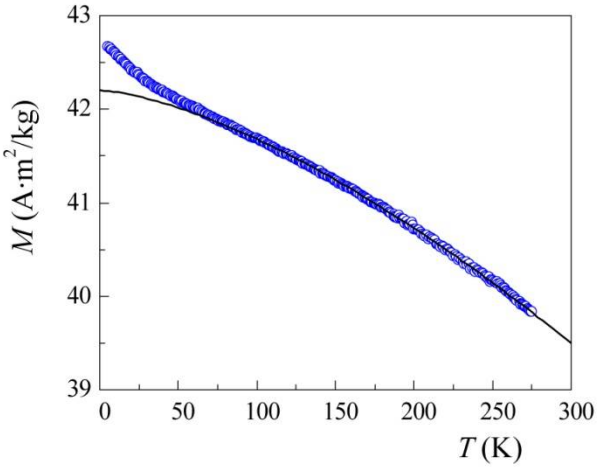

Fig.6 Temperature dependences of magnetization for as-prepared particles at 5 T. Solid line – Eq.3.

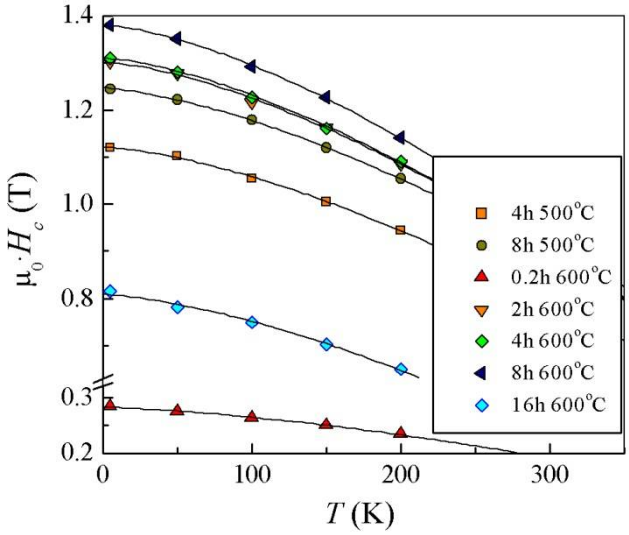

Fig. 7 Temperature dependence of the coercivity in CoPt nanostructured particles, solid line – $H_c \sim H_{c0} \cdot (1\text{-}C \cdot T^{3/2})$.